

## Extremely Low Astigmatism and Aspect Ratio in 650nm-Band Self-Pulsing AlGaInP Lasers with Strained-Quantum-Well Saturable-Absorbing Layer

Hideto ADACHI, Isao KIDOGUCHI, Toshiya FUKUHISA, Kiyotake TANAKA, Masaya MANNOH, and Akira TAKAMORI  
 Semiconductor Research Center, Matsushita Electric Industrial Co., Ltd.  
 3-1-1 Yagumo-Nakamachi, Moriguchi, Osaka 570, Japan

650nm-band self-pulsing lasers which exhibit extremely low astigmatism (2 $\mu$ m) and aspect ratio (2.6) were successfully demonstrated by using carrier-photon interaction in a strained-quantum-well saturable-absorbing layer for the first time. The lasers have advantages for optical focusing as well as low intensity noise up to high temperature.

### 1. INTRODUCTION

AlGaInP lasers are expected to become the next key devices for optical disc systems due to its shorter wavelength<sup>1)</sup>. One practical problem is intensity noise caused by the optical feedback from the disc. Self-sustained pulsation is effective for low noise because of the suppression of mode competition in multi-longitudinal mode oscillation. In the past, self-pulsing AlGaInP laser has been realized by using absorber region in the lateral tails of the optical mode<sup>2-4)</sup>. However, this laser had some disadvantages, i.e., the large astigmatism (over 10 $\mu$ m) and the large aspect ratio (over 4). On the contrary to the lasers, self-pulsing lasers with a saturable absorbing layer are suitable for optical pick-up systems due to its small astigmatism and aspect ratio<sup>5)</sup>. Recently, we have proposed a novel AlGaInP laser structure which has a highly doped SA layer in p-type cladding layer<sup>6)</sup>. By optimizing the design of the layer structure, low astigmatism and low aspect ratio as well as low intensity noise can be expected, simultaneously. In this paper, we report self-pulsing lasers with extremely low astigmatism and aspect ratio by optimizing optical confinement and compressive strain in the SA layer.

### 2. DESIGN AND LASER STRUCTURE

In the case of the laser structure of Ref. 6, an aspect ratio was about 3.0 because an optical confinement factor in the SA layer was designed to be 1.5% in order to realize

self-pulsation even at high temperature. In this work, the optical confinement in the SA layer was designed to be 1.0% in order to realize low aspect ratio and astigmatism. To compensate the decrease of optical confinement, optical absorption effect must be increased by introducing a large compressive strain in the SA layer. The compressive strain enhances the pulsation characteristics because of large optical absorption and large differential gain characteristics in the SA layer.

Saturable absorption characteristics strongly depends on the strain of the SA layer. The strain has an effect on the optical absorption characteristics in the SA layer due to higher InP mole fraction. To investigate the dependence, seven samples with different compressive strain in the SA layer were prepared. The strain in the active layer was +0.50%. Experiments were performed by measuring the current vs. optical output power characteristics at 25°C. Figure 1 shows the relation between the compressive strain in the SA layer and the threshold current. As increasing the strain, the threshold current becomes high due to large optical absorption efficiency. No absorption was found in the sample with the strain of +0.36%. Self-sustained pulsations were observed in the compressive strain more than +0.55% at 25°C. In this work, large compressive strain of +0.77% was adopted to the SA layer. This design will realize a stable self-sustained pulsation characteristics and lower threshold current, simultaneously.

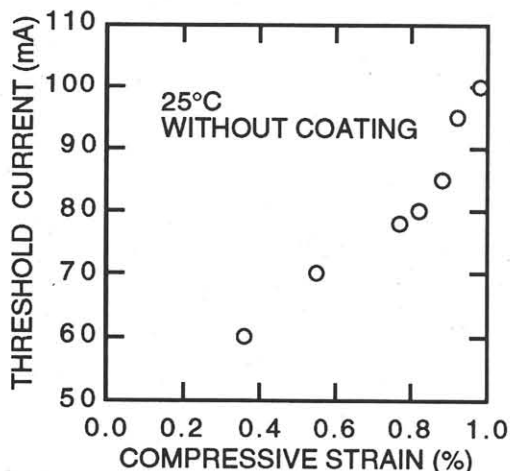


Fig. 1. Relationship between the compressive strain in the SA layer and the threshold current at 25°C.

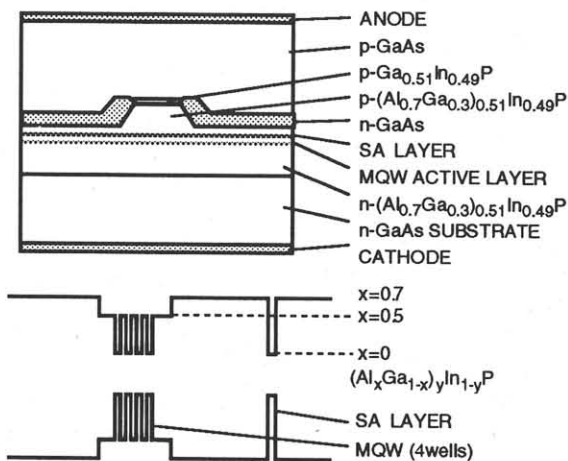


Fig. 2. Schematic cross section and band diagram of the self-pulsing AlGaInP visible laser diodes.

A schematic cross section of the laser structure is shown in Fig. 2. A double heterostructure was based on that of the Ref. 6. The epitaxial growth of the laser structure was carried out on misoriented (100) n-GaAs substrate by low pressure MOVPE. A double heterostructure consists of the following layers: an n-GaAs buffer layer, an n-(Al<sub>0.7</sub>Ga<sub>0.3</sub>)<sub>0.51</sub>In<sub>0.49</sub>P cladding layer (1.1 $\mu$ m), an undoped multiple quantum well (MQW) active layer, a first p-(Al<sub>0.7</sub>Ga<sub>0.3</sub>)<sub>0.51</sub>In<sub>0.49</sub>P cladding layer, the SA layer, a second p-(Al<sub>0.7</sub>Ga<sub>0.3</sub>)<sub>0.51</sub>In<sub>0.49</sub>P cladding layer (0.9 $\mu$ m), a p-Ga<sub>0.51</sub>In<sub>0.49</sub>P layer, and a p-GaAs capping layer. The band diagram of the MQW active layer and the SA layer also shown in Fig. 2. Al and In compositions are denoted by x and 1-y, respectively. The MQW active layer consists of three GaInP strained quantum wells separated by (Al<sub>0.5</sub>Ga<sub>0.5</sub>)<sub>0.51</sub>In<sub>0.49</sub>P barriers. The SA layer consists of a p-GaInP strained quantum well ( $p=2\times 10^{18}\text{cm}^{-3}$ ). The compressive strain of the active layer and the SA layer are +0.50% and +0.77%, respectively. A mesa of the stripe was preferentially buried by an n-GaAs current blocking layer. Finally, a p-GaAs contact layer was overgrown. The refractive index step difference between the inside of the ridge stripe and outside was controlled by the thickness of the first p-cladding layer. In this structure, the refractive index step difference was designed to be  $2.2\times 10^{-2}$ . The index step is large enough so that the optical mode spreading is negligible outside the ridge stripe. The width of the ridge stripe was 4.8 $\mu$ m. We fabricated the lasers with the cavity length of 500 $\mu$ m. The reflectivity of both facets were controlled to be 46%.

### 3. RESULTS AND DISCUSSIONS

The output power versus injection current characteristics was shown in Fig. 3. The abrupt transition in low temperature at low power level is originate in an optical absorption effects. The threshold current at 25 $^{\circ}\text{C}$  was 72.5mA, and the operation current was 85mA at 5mW. The lasing wavelength was 659nm. Far field pattern at 5mW was shown in Fig. 4. The beam divergence angle perpendicular to the junction plane and parallel were 25.1 $^{\circ}$  and 9.7 $^{\circ}$ , respectively, resulting in small aspect ratio of

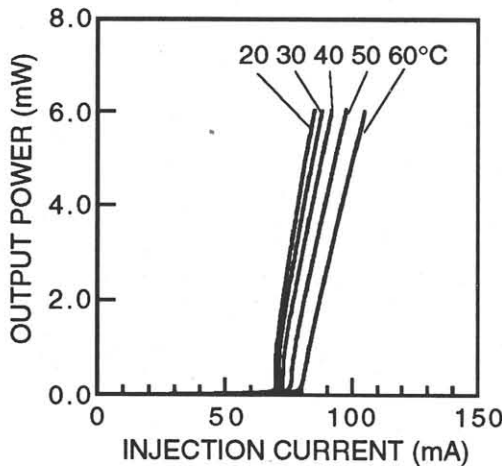


Fig. 3. Output power vs. injection current characteristics of the self-pulsing laser with the saturable absorbing layer. The measurement was performed at 0-60 $^{\circ}\text{C}$ .

2.6. The power dependence of the astigmatism is shown in Fig. 5. The closed circles show the astigmatism of the self-pulsing laser with the strained-quantum-well SA layer. Extremely low astigmatism (below 2 $\mu$ m) was obtained at 5mW. These characteristics were realized by designing the low optical confinement in the SA layer, which is 1.0%. For comparison, the astigmatism of conventional self-pulsing laser with the refractive index step of 0.003<sup>3)</sup> is also shown in Fig. 5. The astigmatism was large due to low optical confinement parallel to the junction plane. We make a list of astigmatism and aspect ratio for the pulsing lasers with 4-well active layer. By reducing the optical confinement factor in the SA layer, low astigmatism and aspect ratio were obtained. Data at the bottom exhibit for the pulsing lasers with the saturable absorption region in the lateral tails of the optical mode.

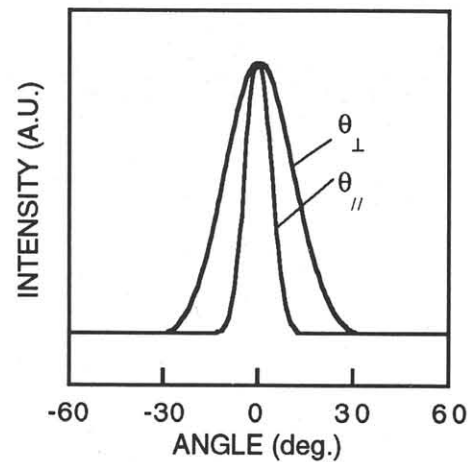


Fig. 4. The beam divergence angle perpendicular to the junction plane and parallel were 25.1 $^{\circ}$  and 9.7 $^{\circ}$ . Small aspect ratio of 2.6 was obtained.

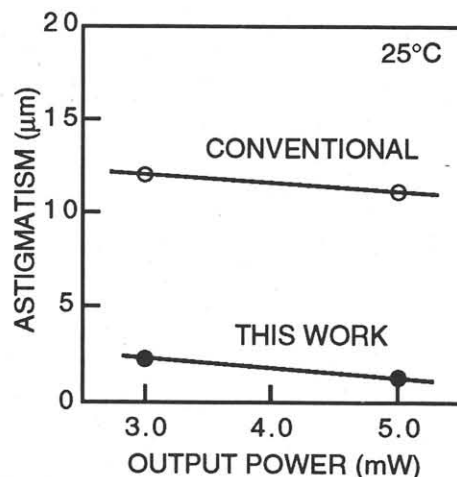


Fig. 5. Power dependence of the astigmatism. The closed circle is for the pulsing lasers with strained-quantum-well SA layer. The open circle is for the conventional pulsing lasers which has the saturable absorbing region in the active layer outside the stripe.

Table 1. Comparison of the astigmatism and aspect ratio. The measurement were performed for the lasers with 4-well active layer.

Confinement* (%)	Astigmatism ( $\mu\text{m}$ )	Aspect ratio
1.0	2	2.6
1.5	4	3.0
- **	$\sim 10$	$>4$

\* Optical confinement factor in the SA layer

\*\* Pulsing laser with saturable absorption region in the lateral tails of the ridge stripe

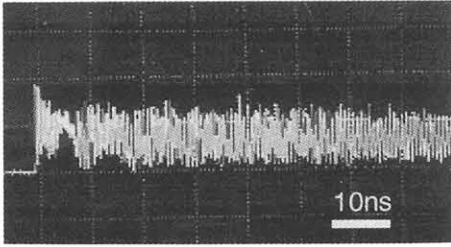


Fig.6. Time dependence of optical output. The measurement was performed at 50°C.

We show in Fig. 6 a plot of the light output versus time from the self-pulsing laser with a DC injection current at 50°C. The temperature dependence of the relative intensity noise (RIN) was measured as shown in Fig. 7. The RIN was below -138 dB/Hz up to 50°C. No mode competition noise was found below 50°C. Thus the oscillation of light output was confirmed in the low RIN range. The self-sustained pulsation characteristics at high temperature was obtained by adopting larger compressive strain in the SA layer than that in the active layer. However, excessive large strain will makes the threshold current and operation current to be large. Consequently, optimization of the strain and the optical confinement is necessary to realize the self-pulsing laser with low astigmatism and aspect ratio.

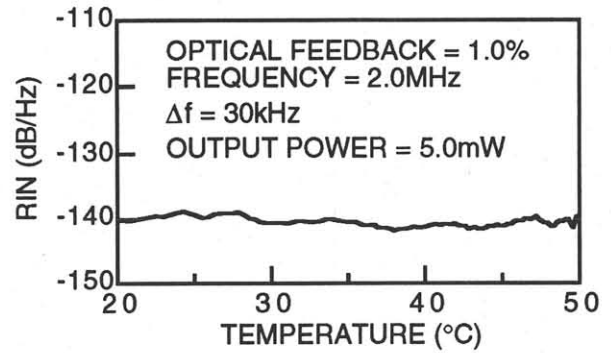


Fig. 7. Temperature dependence of the relative intensity noise (RIN). Mode competition noise was found over 50°C.

#### 4. CONCLUSIONS

Extremely low astigmatism and aspect ratio, as well as low intensity noise, were obtained in the self-pulsing lasers with the strained-quantum-well SA layer. 500- $\mu\text{m}$ -long devices were fabricated, resulting in the small astigmatism of 2 $\mu\text{m}$  and small aspect ratio of 2.6. It is realized by optimizing optical confinement and compressive strain in the SA layer. The relative intensity noise (RIN) was below -138 dB/Hz in the temperature ranging from 20 to 50°C at the output power of 5mW.

#### Acknowledgments

The authors wish to thank T. Kawata, and T. Ohnishi for their considerable support. We also thank K. Ohnaka, T. Onuma for their instructive suggestions and encouragement.

#### References

- 1) M. Mannoh, J. Hoshina, S. Kamiyama, H. Ohta, Y. Ban, and K. Ohnaka, *Appl. Phys. Lett.* **62** (1993) 1173.
- 2) M. Yamada, *IEEE J. Quantum Electron.* **29** (1993) 1330.
- 3) H. Adachi, S. Kamiyama, and I. Kidoguchi, *Optical and Quantum Electronics* **28** (1996) 541.
- 4) Y. Bessho, T. Uetani, R. Hiroyama, K. Komeda, M. Shono, A. Ibaraki, K. Yodoshi, and T. Niina, *Electron. Lett.* **32** (1996) 667.
- 5) R. C. P. Hoskens and T. G. van de Roer, *Appl. Phys. Lett.* **67** (1995) 1343.
- 6) H. Adachi, S. Kamiyama, I. Kidoguchi, and T. Uenoyama, *IEEE Photon. Technol. Lett.* **7** (1995) 1406.